JOURNAL OF Materials CHEMISTRY

Electrosynthesis and analytical characterisation of polypyrrole thin films modified with copper nanoparticles†

Nicola Cioffi,[a] Luisa Torsi,*[a] Ilario Losito,[a] Cinzia Di Franco,[a] Isabella De Bari,[a] Luca Chiavarone,[b] Gaetano Scamarcio,[b] Vessela Tsakova,[c] Luisa Sabbatini[a] and Pier Giorgio Zambonin[a]

[a]*Dipartimento di Chimica, Università degli Studi di Bari, 4, via Orabona, I-70126 Bari, Italy. E-mail: torsi@chimica.uniba.it*
[b]*Dipartimento di Fisica, Università degli Studi di Bari, 4, via Orabona, I-70126 Bari, Italy*
[c]*Institute of Physical Chemistry, Bulgarian Academy of Science, 1040 Sofia, Bulgaria*

Received 8th December 2000, Accepted 13th February 2001
First published as an Advance Article on the web 13th March 2001

Copper–polypyrrole (Cu–PPy) composites have been synthesised following an all-electrochemical procedure comprising the deposition of a thin PPy film and the subsequent pulsed potentiostatic deposition of copper from a $CuCl_2$ solution. Surface and bulk characterisation of the specimens has been carried out using X-ray Photoelectron and Micro-Raman spectroscopies, respectively. Cyclic voltammetry has been used to investigate electroactive species and copper–polypyrrole interactions in the materials. Composite morphology has been assessed by Scanning and Transmission Electron Microscopies. The cluster size depended upon the amount of copper deposited; for a copper loading of 44 mC cm^{-2}, clusters with a mean diameter of 160 nm were deposited. These clusters are mainly composed of Cu_2O, although chloride species and CuO were found on the surface of the composites. Evidence is provided that Cu–N complexes were formed too.

Introduction

Metal–polymer nanostructured composites are giving rise to a great deal of interest because of their possible applications in technologically relevant fields, such as electrocatalysis and sensors.[1–9] All-electrochemically produced metal-modified polymer films have been already proven to hold promising properties as active layers in gas sensors capable of operating at room temperature.[10]

Different procedures have been used so far for the fabrication of such organic/inorganic systems, amongst which Pulsed Electro-Deposition (PED) has been widely employed to modify the electrical and electrochemical properties of the polymer substrate since its first use reported by Yassar *et al.*[11] The main advantage of this technique is to achieve reductive electrodeposition of metallic species from a solution of their cations, minimising the conductivity loss of the polymer. Moreover it allows control over the loading and the size of the inorganic particles.[12,13]

The present paper deals with the electrochemical synthesis and detailed analytical characterisation of copper–polypyrrole (Cu–PPy) composites obtained by depositing copper clusters from an acidic $CuCl_2$ solution on a previously electrosynthesised PPy thin film. Chloride containing solutions, although being systems with a fairly complicated electrochemistry in the presence of copper cations, allow the deposition of Cu(I) species, mainly as Cu_2O;[14] cathodic deposition from Cu_2SO_4 leads, in contrast, mainly to Cu(0).[15] Since Cu_2O and PPy have well recognised catalytic and electrocatalytic activities,[1,16] it is of interest to find a way to prepare Cu–PPy nanostructured composites where most of the copper is present as Cu_2O. Recently, a study of copper deposition from a chloride containing solution on a poly-3-methylthiophene (P3MT) polymer has been published.[13] In the present paper PPy is used instead of P3MT as the organic matrix because the E_0 (equilibrium potential) of the former is more negative than that of the latter. As a result, the Cu(I)–PPy system is expected to be more stable than Cu(I)/P3MT.

Experimental

Pyrrole (Py), purchased from Aldrich, was purified by vacuum distillation and stored under nitrogen at −27 °C. All other chemicals were ACS reagent grade and used without any further purification. The solutions were prepared using triply distilled water and deoxygenated by bubbling nitrogen. Platinum rods (3 mm diameter) and sheets were purchased from Goodfellow and had a purity of 99.95%.

Electrochemical experiments were performed using an EG&G Princeton Applied Research 263 Potentiostat–Galvanostat and conventional three electrode cells. Disk working electrodes (disk area 0.083 cm^2) for cyclic voltammetry (CV) were obtained by press-fitting a Pt rod into a Teflon tube. Pt sheets (area *ca.* 1 cm^2) were used as counter electrodes in all the electrochemical experiments and as substrates of the Cu–PPy samples employed for the spectroscopic and Scanning Electron Microscopy (SEM) characterisations. Before use Pt electrodes were polished and pre-treated as reported elsewhere.[17] An Ag/AgCl,KCl(sat) electrode (−45 mV *vs.* Saturated Calomel Electrode) was used as reference.

Cu–PPy films were deposited on Pt or on Indium Tin Oxide (ITO)-covered glass electrodes using a two-step procedure. Firstly polypyrrole (PPy) films were potentiostatically deposited at +0.7 *vs.* reference from an aqueous solution containing Py 0.4 M and KCl 0.1 M, under a nitrogen atmosphere. PPy thickness, estimated from coulometric measurements of the polymerisation charge density,[18] was 60 nm unless otherwise stated. The second step was a pulsed potentiostatic deposition

†Electronic supplementary information (ESI) available: experimental and Poisson distributions of the distances between 1st, 2nd and 3rd neighbouring crystals. See http://www.rsc.org/suppdata/jm/b0/b009857o/

 DOI: 10.1039/b009857o

of copper from a $CuCl_2$ 0.1 M, KCl 0.1 M solution (pH = 5). The pulses had the following voltage sequence: 0 V, −0.350 V, 0 V *vs.* reference, each step lasting 4 ms. The copper loading, expressed as electrodeposition charge density, varied from 17 to 340 mC cm^{-2}, approximately corresponding to a deposition time of 1.5–20 s or, equivalently, to 125–1670 pulses. The charge density exclusively due to PPy reduction was estimated to be negligible with respect to that of copper deposition by performing blank pulsed experiments on PPy films in the supporting electrolyte solution. Immediately after being synthesised, Cu–PPy film electrodes were washed with triply distilled water and subjected to *ex situ* characterisation.

The electrochemical characterisation of as deposited Cu–PPy samples was performed using the composite film as the working electrode in a CV experiment carried out in KCl 0.1 M solution. The starting potential was set at −25 mV *vs.* reference; this value was chosen *ad hoc* since it was very close to the open circuit potential of the composite film in the supporting electrolyte.

In order to perform Transmission Electron Microscopy (TEM) analysis on a self-standing Cu–PPy film, the composites were directly synthesised onto ITO-glass electrodes. As a matter of fact the Cu–PPy films could be easily removed from the ITO substrate[19] and then sandwiched between two 200 mesh copper grids. Transmission electron micrographs were produced at 100 KV under a Philips-400 T microscope.

SEM characterisation and Energy Dispersive X-ray (EDX) qualitative analysis were carried out with a Cambridge Stereoscan 240 coupled to a microanalysis system (Link AN10000).

Micro-Raman analysis was performed with a Dilor LabRam I spectrometer/microscope comprising a single 32 cm monochromator, a holographic notch filter, a cofocal microscope—which allowed laser focussing to a minimum size of less than 1 μm—and a CCD detector. The 632.8 nm line of an He–Ne laser was used for the excitation.

X-Ray Photoelectron Spectroscopy (XPS) measurements were performed using a Leybold LHS10 spectrometer equipped with an unmonochromatised MgKα source. The pressure in the analysis chamber varied in the 10^{-8}–10^{-9} mbar range. Survey spectra (fixed retarding ratio, $B = 3$) and high-resolution spectra (fixed analyser transmission, $E_0 = 50$ eV) for C1s, O1s, Cu2p, $CuL_3M_{45}M_{45}$, N1s, Cl2p regions were collected. Calibration of the spectra was performed by taking the intracyclic pyrrolic nitrogen component of the N1s electron peak (binding energy = 399.6 eV) as internal reference.[20] Data analysis was performed as reported in ref. 20. The modified Auger parameter (α′) for Cu was calculated by adding the binding energy (BE) for the $Cu2p_{3/2}$ signal to the maximum kinetic energy (KE) of the $CuL_3M_{45}M_{45}$ Auger signal. The fitting of the $Cu2p_{3/2}$ spectral region was performed starting from a linear background subtraction instead of a non-linear routine (Shirley algorithm) in order to avoid truncation of the shake-up signals at higher BE. The full width at half maximum (FWHM) values used to fit the $Cu2p_{3/2}$ region and the $CuKL_{23}L_{23}$ signal were derived from a previous analysis of CuO and Cu_2O standards.

Results

Surface analysis

In Fig. 1A the $Cu2p_{3/2}$ XPS spectrum recorded for a Cu–PPy sample with a copper loading of 300 mC cm^{-2} is reported. Five peaks were employed to fit the experimental curve. The lower binding energy peak (BE = 932.3 eV, FWHM = 1.5 eV) is attributed, on the basis of the modified Auger parameter (α′ = 1848.7 eV), to Cu(I) species; this attribution allows us to assess that—at least on the surface of the sample—no metallic copper is present. The fitting of the Cu(II) component was

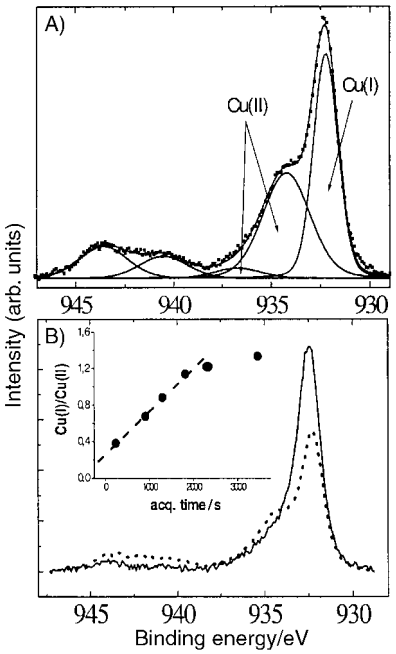

Fig. 1 (A) High resolution XPS spectrum of $Cu2p_{3/2}$ region of a Cu–PPy sample (PPy 60 nm thick, Cu loading: 300 mC cm^{-2}). (B) Comparison between the $Cu2p_{3/2}$ spectrum recorded at the beginning of the acquisition (dotted line) and after one hour of acquisition (continuous line). In the inset: evolution of the Cu(I)/Cu(II) peak intensity ratio.

obtained with two peaks centred at 934.5 and 937.0 eV (both having a FWHM of 2.8 eV), while the tail at high binding energy, typical of the shake-up signals of Cu(II) compounds, has been fitted with peaks centred at 940.0 and 943.2 eV (both having a FWHM of 2.9 eV). The presence of both oxygen and chloride signals in the XPS spectrum implies that species such as Cu_2O and CuCl, as well as CuO and $CuCl_2$, could be present on the Cu–PPy samples. For each copper oxidation state, an unambiguous assignment to oxide and/or chloride copper species relying only on the XPS chemical shift cannot be done, since the differences in the peak positions of the different compounds are lower than the spectral resolution.

In Fig. 1B a comparison is reported between the $Cu2p_{3/2}$ signals recorded for the same sample at the very beginning of the spectrum acquisition (dotted line) and after 1 hour exposure to X-ray photons (continuous line). It is apparent that a modification of the spectrum occurred because of the transformation of Cu(II) species into Cu(I) ones. This sample alteration seems to be correlated to the highly dispersed nature of Cu species in the polymer matrix. Analysis performed with the same XPS apparatus on standard CuO powder did not exhibit any transformation even when exposed to X-rays for a longer time,[21] while the same degradation effect was observed when exposing copper oxides dispersed in inorganic matrices.[22] The mechanism originating this transformation is not clear although heating related effects could be involved.

In order to follow the kinetics of this process, several spectra were recorded at different time intervals. The ratio between the areas of the Cu(I) and Cu(II) components is shown to increase with time in the inset of Fig. 1B. An extrapolation of the data in the linear portion of the plot allows us to say that the elicited ratio is significantly different from zero at the beginning of the experiment meaning that, even at the surface of a pristine Cu–PPy sample, a quantifiable amount of Cu(I) is present.

Fig. 2 displays a comparison between the N1s XP signals recorded for an as-synthesised PPy thin film (Fig. 2A) and a film subjected to a "dummy" copper deposition (Fig. 2B); *i.e.* a film subjected to the pulse program used for the copper depositions, but while immersed in bare supporting electrolyte

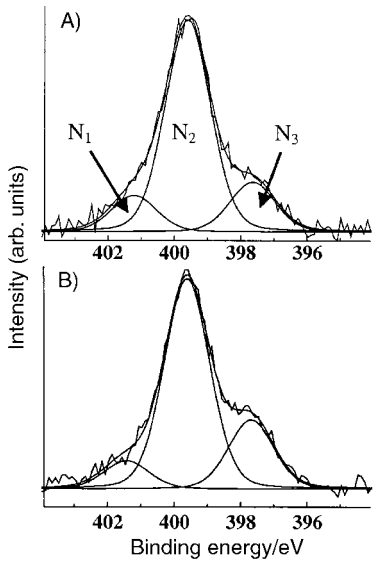

Fig. 2 High resolution XPS spectra of N1s region for A) pristine PPy film; B) PPy film subjected to a series of negative pulses in supporting electrolyte (see text).

solution. The "dummy" deposition lasted for a time longer than that needed to achieve the highest copper loading (340 mC cm^{-2}). The attribution of the N1s components is given as follows:[20] N_1 (BE = 401.3 eV, FWHM = 1.6 eV) is due to the charged polaronic nitrogens, N_2 (BE = 399.6 eV, FWHM = 1.6 eV) is the pyrrolic nitrogen (–NH–), while N_3 (BE = 397.7 eV, FWHM = 1.6 eV) is due to the iminic (–C=N–) deprotonated component. The comparison of the N1s spectra reported in Fig. 2A and B shows that only slight modifications occurred. In particular the N_1 component decreases, while the N_3 increases. It has been already demonstrated that upon electrochemical or chemical doping of PPy the N_1 component increases, while upon reduction, as well as upon chemical deprotonation in NaOH, N_3 increases.[23] It can be derived that the pulsed potentiostatic program causes a slight reduction of PPy, with an eventual lowering of its conductivity.

In Fig. 3 the dependence of the N1s signal of Cu–PPy samples upon the amount of deposited copper is presented. In

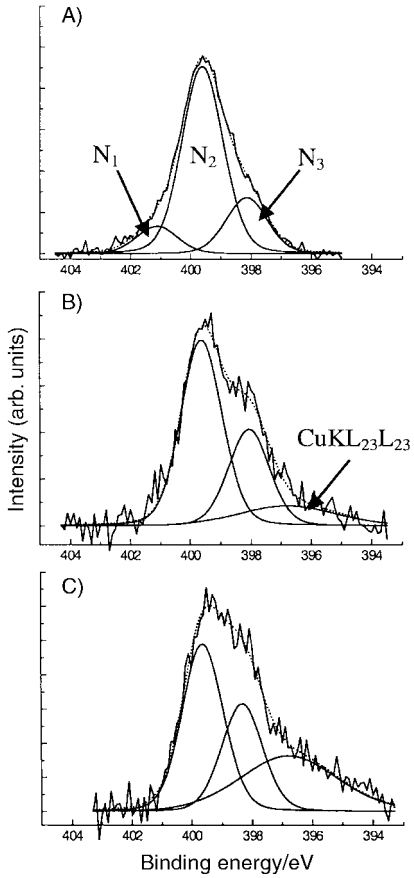

Fig. 3 Comparison between the high resolution XPS spectra of the N1s region for Cu–PPy composites (PPy 60 nm thick) with different copper loadings: A) 17 mC cm^{-2}; B) 108 mC cm^{-2}; C) 200 mC cm^{-2}.

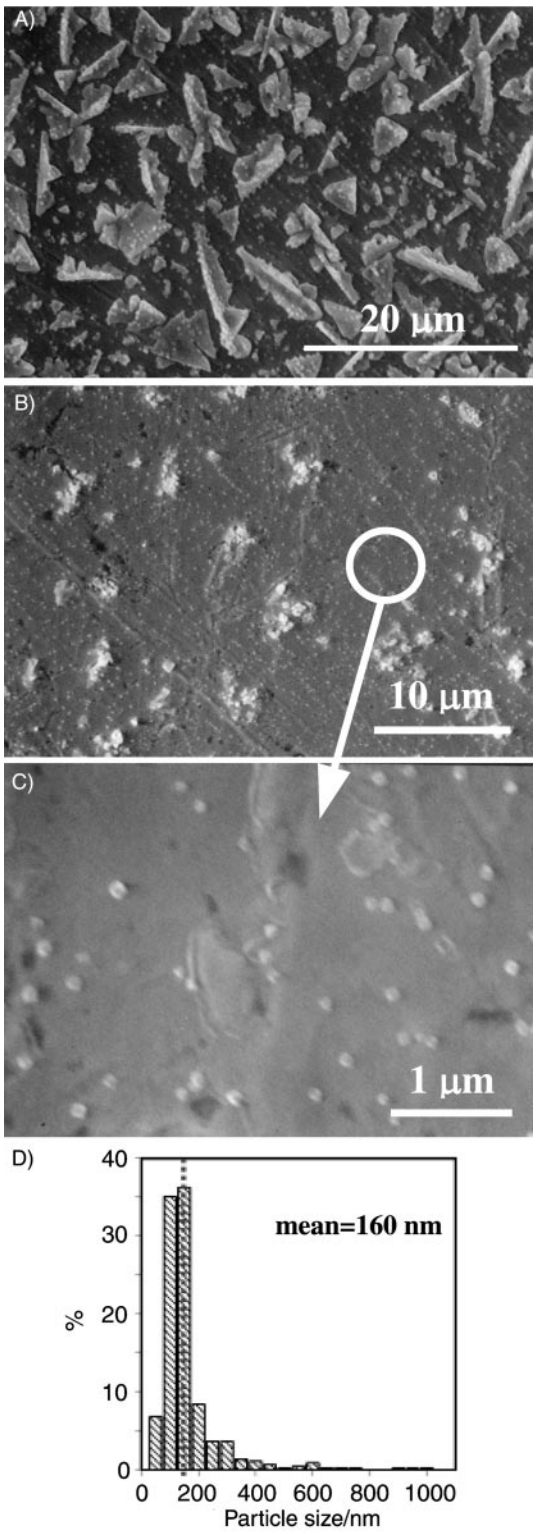

Fig. 4 SEM micrographs of PPy films (60 nm thick) with different copper loadings: A) 340 mC cm^{-2}; B) 44 mC cm^{-2}; C) magnification of the highlighted area in part B; D) size distribution of the clusters of part B, obtained on more than 500 particles.

particular, the spectra of samples with copper contents corresponding to deposition charge densities of 17 mC cm^{-2}, 108 mC cm^{-2} and 200 mC cm^{-2} are reported in Fig. 3A, B and C, respectively. A pronounced decrease of N_1 and an increase of N_3 occur upon copper inclusion; these changes are too large to be exclusively interpreted as an effect of reduction due to the negative pulses. The progressive PPy surface reduction upon copper deposition could also be a consequence of the electron transfer from the copper crystals to the PPy matrix, which is energetically favoured, since the electrochemical potential of oxidised PPy[24] is less negative than that of Cu(0)/Cu(I). The increase of the intensity of the iminic nitrogen (N_3) observed at high copper loading could be due to the occurrence of an interaction between the deposited copper and the electron rich nitrogen. This hypothesis is also supported by the electrochemical characterisation reported later in the text. However, it is important to outline that the intensity in the low BE region of the spectrum increases also because of the appearance of a secondary Cu Auger signal ($CuKL_{23}L_{23}$, BE = 396.8 eV, FWHM = 3.8 eV).

Morphological characterisation

In Fig. 4 SEM micrographs of PPy films loaded with different amounts of copper are shown. For high copper loading (340 mC cm^{-2}, Fig. 4A), the deposit is mainly made of lanceolate crystals several microns long and a few microns wide. When the copper loading is almost one order of magnitude lower (44 mC cm^{-2}, Fig. 4B), the clusters are much smaller and several round shaped features can be seen (Fig. 4C). In the latter case, the mean diameter of the clusters is 160 nm (see Fig. 4D). The EDX qualitative analysis reveals that the clusters—both in Fig. 4A and B—are composed of Cu, O and Cl, and are, therefore, attributed to copper deposits. The darker and flatter regions are composed of N, O, C, and traces of Cu, and are therefore attributed to uncovered PPy portions of the sample.

A statistical analysis of the surface distribution of the copper clusters shown in Fig. 4B was performed by measuring the distances between closest neighbouring crystals. Thus data for the distances between first, r_1, second, r_2 and third, r_3 neighbours were obtained and the experimental probability distributions $dP_1(r_1)$, $dP_2(r_2)$, $dP_3(r_3)$ to find the corresponding (first, second or third) neighbour of a given crystal at a given distance were calculated. Data for the mean values $r_{1,mean}$, $r_{2,mean}$ and $r_{3,mean}$ and the standard deviations σ_1, σ_2, σ_3 of these quantities are summarised in Table 1. Theoretical histograms corresponding to the case of a completely random, Poissonian distribution of the metal clusters were easily calculated by means of a single parameter, the average number N of deposited crystals using the formulae:[25]

$$dP_1(r_1) = 2\pi r_1 N \exp(-\pi r_1^2 N) dr_1 \quad (1)$$

$$dP_2(r_2) = 2\pi^2 r_2^3 N^2 \exp(-\pi r_2^2 N) dr_2 \quad (2)$$

$$dP_3(r_3) = \pi^3 r_3^5 N^3 \exp(-\pi r_3^2 N) dr_3 \quad (3)$$

A good correspondence between experimental and Poissonian distributions was found.† Additional evidence in this respect is given by the values of the σ/r_{mean} ratios (see Table 1),

Table 1 Mean values and standard deviations relevant to the distances between the first, second, third neighbouring crystals in Fig. 4B. In the last column is reported the theoretical σ_n/r_n ratio expected in the case of a Poissonian distribution of the copper clusters in the composite

n	$r_{n,mean}$/μm	σ_n/μm	$\sigma_n/r_{n,mean}$	$\sigma_n/r_{n,mean}$, Poissonian[26]
1	0.391	0.184	0.484	0.523
2	0.579	0.207	0.357	0.364
3	0.777	0.236	0.304	0.295

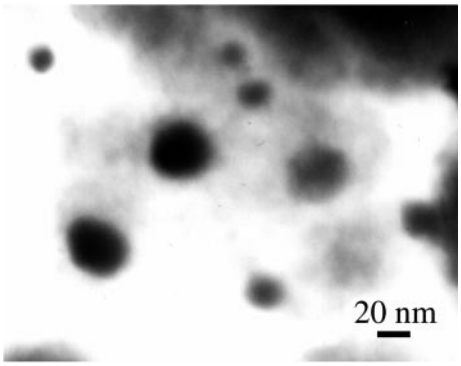

Fig. 5 TEM micrograph of a Cu–PPy sample having a PPy thickness of 60 nm and a copper loading of 44 mC cm^{-2}.

which are close to the theoretical ones.[26] These results should not be considered as a trivial finding. Indeed, a marked deviation from Poissonian behaviour was observed in the case of copper inclusions potentiostatically deposited in a reduced thin polyaniline layer.[27] This was attributed to the mutual influence of the available metal clusters in the nucleation and growth stage. As a consequence not all of the available active sites for metal deposition have been really occupied by metal clusters.[27] The Poissonian behaviour found in the present case is an indication of the absence of any limitations on the nucleation and growth rates imposed by the mutual influence of existing neighbouring clusters. This should be attributed to the pulse deposition procedure used in this study allowing very probably any concentration and potential gradients arising in the vicinity of already existing growing crystals to level out.

In Fig. 5 a TEM photograph taken directly on a Cu–PPy thin film (copper loading 44 mC cm^{-2}) is reported. The bright parts of the picture originate from the electron transparent thin PPy film, while the dark round regions are associated with the copper inclusions. From this micrograph it is clear that besides larger clusters, also inclusions with a diameter as small as 20 nm are present.

Microprobe-Raman spectra

The high spatial resolution (< 1 μm) of the microprobe Raman set-up used has been exploited to assess the bulk chemical composition of selected sample regions. Fig. 6 shows Raman spectra representative of Cu clusters (trace A) and the PPy matrix (trace B), recorded with He–Ne laser excitation. This laser line was used since all the compounds possibly present in the Cu–PPy samples (PPy, CuO, Cu_2O, CuCl and $CuCl_2$) are

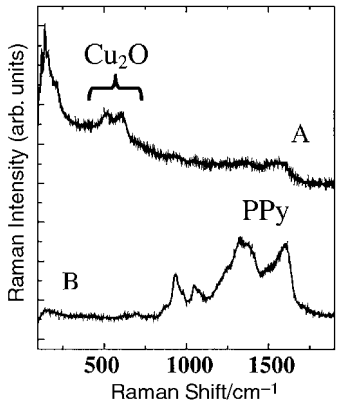

Fig. 6 Microprobe-Raman spectra of a Cu–PPy sample (PPy 60 nm thick, copper loading: 340 mC cm^{-2}) excited with the 632.8 nm He–Ne laser line. A) Laser spot focused on a Cu cluster region; B) laser spot focused on a PPy region.

transparent to the excitation at 632.8 nm. In the 100–1000 cm^{-1} wavenumber range, trace (A) shows a series of sharp peaks around 150 cm^{-1} and two broad bands at 513 and 602 cm^{-1}, characteristics of Cu_2O.[28] Trace (B) is dominated by a series of bands at 943 cm^{-1}, 1043 cm^{-1}, 1329 cm^{-1} and 1606 cm^{-1}, associated with the vibrations of PPy.[29] When the Cu clusters were excited with phonons resonant with the CuO band-gap,[30] namely the 482.5 nm laser line of a Kr^+ laser, the resulting Raman spectrum showed both the Cu_2O and CuO phonons. This demonstrates that a very small quantity of Cu(II) oxide is present, which can be evidenced only by exploiting resonance enhancement of the Raman signal. This finding, combined with the XPS data, allows us to attribute the Cu(II) species detected on the material surface to CuO.

The presence of the peak at 1606 cm^{-1} (attributed to the $\nu_{C=C}$ vibration mode) in the Raman spectrum of the PPy flat region of Fig. 6B, is strongly suggestive of extensive doping of the matrix.[31] This is apparently in contrast with the analysis of the N1s XPS spectrum. A possible explanation for this discrepancy can be given considering the different surface sensitivity of the two techniques. Raman spectroscopy gives information on bulk PPy which is less affected by the reducing action of copper deposition on the surface.

Electrochemical characterisation

Table 2 summarises the positions and the intensities the peaks, along with the relevant electrochemical processes, occurring when a Pt electrode or an as-synthesised PPy film (1.5 μm thick) is cycled in the copper electroplating solution ($CuCl_2$ 0.1 M, KCl 0.1 M).[32] The peaks relevant to PPy redox activity are not listed because the currents involved are much lower than those due to copper species. The redox couples labelled in the table as A–F and B–E are observed on both Pt and PPy-modified platinum electrodes. They have been respectively attributed to Cu(0)/Cu(I) and Cu(I)/Cu(II) one-electron processes, the Cu(I) oxidation state being stabilised at the pH of the deposition medium and by the presence of chloride anions. The redox couple C–D is only observed on PPy-modified platinum electrodes. Moreover, the current density of peaks C and D increases with the thickness of the PPy film. Such a dependence cannot simply be ascribed to an enhancement of the electrode area, since a similar increment should also be observed for the other peaks (see for instance peak B). A redox process involving a complex between the deposited copper and polypyrrole could occur under peaks C,D. Moreover, since the C,D peak potential values are more positive than those relevant to insoluble Cu(I) species (Cu_2O and or CuCl), a particularly stable Cu(I)–PPy compound should be involved in the redox process.

Fig. 7 reports the first cycle of two cyclic voltammograms relevant to composites having the same copper loading

Table 2 Positions, current peak densities and attributions of the electrochemical peaks appearing when a Pt electrode or an as-synthesised PPy film is cycled in the copper electroplating solution ($CuCl_2$ 0.1 M, KCl 0.1 M), between −500 and 700 mV. Asterisks indicate a new hypothesised Cu(I) species

	Peak potential/ mV (*vs.* reference)		Peak current density/ mA cm^{-2}		
Peak	Pt	PPy	Pt	PPy	Process
A	150–200	100	26	16	Cu(0)→Cu(I)
B	500	550	34	35	Cu(I)→Cu(II)
C	—	700–750	—	⩽0.6	Cu(I)*→Cu(II)
D	—	450–500	—	3	Cu(II)→Cu(I)*
E	50	−60	8	3	Cu(II)→Cu(I)
F	−300	−400	20	21	Cu(I)→Cu(0)

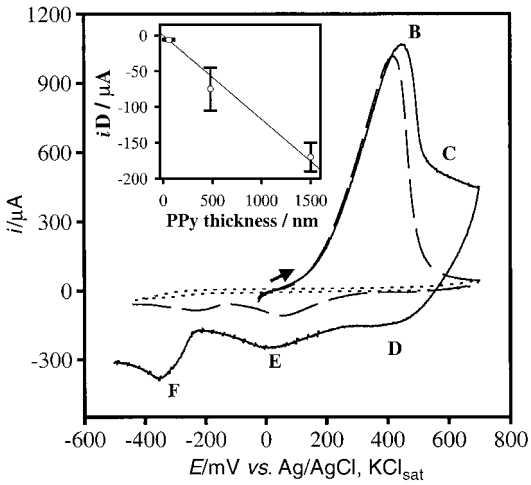

Fig. 7 First cycle of two cyclic voltammograms carried out in KCl 0.1 M and relevant to composites having the same copper loading (170 mC cm^{-2}) but different PPy thickness (dashed line 60 nm, continuous line 1.5 μm). Dotted line curve is the CV response of a pristine, 60 nm thick, PPy film cycled in the same supporting electrolyte. The arrow indicates the scan direction. In the inset: dependence of the current intensity of peak D upon PPy thickness (each point is the average of three replicates).

(170 mC cm^{-2}) but different PPy thickness (dashed line 60 nm, solid line 1.5 μm). The experiments were carried out cycling the Cu–PPy working electrodes in supporting electrolyte. In both cases the starting potential was fixed at −25 mV in order not to reduce or oxidise the copper species present in the as-prepared composites. The very low current values recorded at the beginning of the sweeps and the absence of an oxidation peak at *ca.* 100 mV allowed us to exclude the presence of Cu(0) in the composites, while the high peak currents read at *ca.* 500 mV (peak B) are in accordance with the spectroscopic information that Cu(I) compounds are the most abundant copper species in the composites. The shoulder (C) falling at *ca.* 650–700 mV and the broad peak D can be attributed to the electrochemistry of the Cu(I)–polypyrrole complex. A variation of the PPy thickness (in the range 60–1500 nm) in composites having a copper loading of 170 mC cm^{-2} allowed us to observe a linear dependence of the current density of peak D upon the PPy thickness, with a slope value of -1.4 mA $cm^{-2} \times \mu m_{PPy}^{-1}$ (see the inset of Fig. 7). Finally, the last two cathodic peaks (E,F) are due to Cu(II) and Cu(I) consecutive reductions. Their intensity is low, as compared to peak B; however this is not surprising since the diffusion of the Cu(II) ions (produced under peak B) from the electrode in the bulk electrolyte solution lowers their concentration at the electrode surface.

The presence of a stable complex in the Cu–PPy film is also confirmed by the experiment reported in Fig. 8, where a Cu–PPy film (PPy 1.5 μm thick, copper loading 170 mC cm^{-2}) was cycled in the supporting electrolyte for a long time; in the figure the seventh to the fifteenth cycles are reported. In this case the positive potential window was extended to +800 mV *vs.* reference in order to better observe peak C. The first cycles (not reported) lead to the dissolution of most of the copper previously deposited, thus allowing the redox process involving lower currents to become visible. As is evident in the figure, even when the intensity of peaks A/F, B/E has been dramatically lowered, the redox couple C/D is still present, confirming the attribution of these peaks to a process involving a Cu(I) species that is tightly bound to the PPy matrix.

Discussion

PED techniques, generally used to prepare micro-[33] and, more recently, also nano-clusters of copper,[12] lead to deposits that

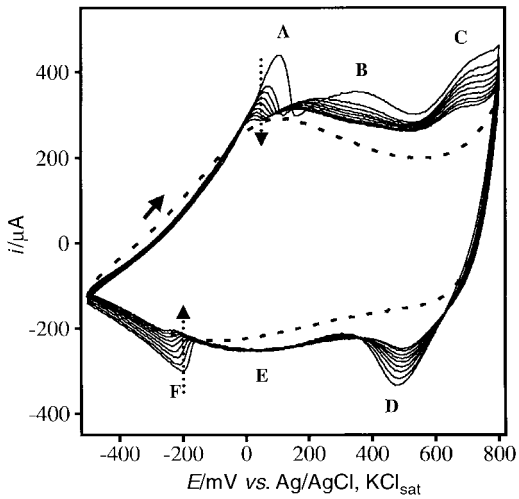

Fig. 8 Continuous line shows the seventh to fifteenth cycles of the CV obtained cycling a Cu–PPy film (PPy 1.5 μm thick, copper loading 170 mC cm^{-2}) in KCl 0.1 M supporting electrolyte. Dotted line is the CV response of a pristine, 1.5 μm thick, PPy film cycled in the same supporting electrolyte. Dotted arrows indicate the current intensity trend, while the solid arrow indicates the scan direction.

can be quite heterogeneous, in that different copper species can be present in the deposit. As far as the samples prepared for the present study are concerned, what is most likely to happen is that during the negative part (−350 mV) of the pulse, Cu(II) species are reduced and, according to the Pourbaix diagram,[34] Cu(0) should be deposited on the electrode. In fact, as already pointed out by Lu *et al.* in a study involving copper deposition from a copper chloride solution on an inorganic substrate,[14] this is not the case, and kinetic considerations lead us to say that both Cu(0) and Cu_2O are to be deposited in the experimental conditions used in the present study. When the potential switches to zero, the only species deposited is Cu_2O.

Electrochemical data confirmed the presence of Cu(I) compounds in the bulk of the crystals, while micro-Raman results allowed us to state that the species constituting the bulk of the crystals was Cu_2O. CuO was also detected in trace amounts. This evidence, combined with the results of the XPS analysis, suggests that Cu(II) species can be attributed to CuO, deriving from surface oxidation due to air exposure of the samples. No presence of Cu(0) has been revealed in the present study. A possible explanation for this evidence can be given considering the lowering of PPy conductivity at negative potentials; this could enhance the overpotential required for reductive pulsed deposition of metallic copper.

As far as the role of chloride is concerned, the morphological study of Lu *et al.*[14] assessed that chloride anions, *via* an adsorption process, force the copper oxide crystals to grow in preferential directions rather than forming copper chloride crystals themselves. As a consequence, Cu_2O crystals grown from chloride solution have the peculiar Y shape exhibited also by the crystals shown in Fig. 4A.

The changes in the N1s XPS signal observed at high copper loadings suggest, at least on the surface of the composites, an interaction between nitrogen and copper. This could be due to direct electron exchange, leading to reduction of the PPy matrix and oxidation of deposited copper, or to a Cu(I) complexation by electron rich nitrogen. Cyclic voltammetry confirmed this second hypothesis, showing the presence of a new redox couple, falling at high positive potentials, attributed to the electrochemistry of a stable Cu(I)–N complex, whose formation has been already reported by Liu and Hwang, who studied the electrochemical dissolution of Cu crystals electrodeposited on PPy from acidic solutions.[35]

Conclusions

In the present paper the electrosynthesis and a detailed analytical characterisation of nanostructured composite thin films of polypyrrole modified with copper inclusions is presented. The pulsed potentiostatic copper deposition on a PPy thin film from a slightly acidic (pH = 5) $CuCl_2$ solution resulted in clusters composed of Cu(I), mainly as Cu_2O. Chloride species, as well as CuO, were present on the surface of the clusters, as traces, but did not affect significantly the bulk composition of the materials. In the case of a copper loading of 44 mC cm^{-2}, the SEM characterisation showed a cluster mean dimension of 160 nm. Electrochemical and XPS evidence of atomically dispersed copper, in the form of nitrogen stabilised Cu(I)–N complexes, was also provided. Possible application of these thin films can be envisaged in the field of gas and electrocatalytic sensors, exploiting the catalytic activity of both polypyrrole and Cu(I) species.[1,10,16]

Acknowledgements

L. Chiavarone, N. Cioffi, I. De Bari and C. Di Franco performed part of the present study during their post-graduate or PhD training. Dr. Teresa Bleve-Zacheo, who performed the TEM analysis, is gratefully acknowledged for her valuable support. Mr. Angelo Tambone is gratefully acknowledged for his skilled help in acquiring the XPS spectra. This work was carried out with the financial support of Ministero della Ricerca Scientifica e Tecnologica (MURST) and Consiglio Nazionale delle Ricerche (CNR).

References

1 A. Malinauskas, *Synth. Met.*, 1999, **107**, 75.
2 M. Hepel, *J. Electrochem. Soc.*, 1998, **145**, 124.
3 Z. Qi and P. G. Pickup, *Chem. Commun.*, 1998, **28**, 15.
4 S. Deki, K. Akamatsu, T. Yano, M. Mizuhata and A. Kajinami, *J. Mater. Chem.*, 1998, **8**, 1865.
5 Y. Li, R. lenigk, X. Wu, B. Gruending, S. Dong and R. Renneberg, *Electroanalysis*, 1998, **10**, 671.
6 I. G. Casella, T. R. I. Cataldi, A. Guerrieri and E. Desimoni, *Anal. Chim. Acta*, 1996, **353**, 217.
7 H. Kim and W. Chang, *Synth. Met.*, 1999, **101**, 150.
8 D. J. Strike, M. G. H Meijerink and M. Koudelka-Hep, *Fresenius J. Anal. Chem.*, 1999, **364**, 499 and references cited therein.
9 B. P. J. de Lacy Costello, P. Evans, R. J. Ewen, C. L. Honeybourne and N. M. Ratcliffe, *J. Mater. Chem.*, 1996, **6**, 289.
10 L. Torsi, M. Pezzuto, P. Siciliano, R. Rella, L. Sabbatini, L. Valli and P. G. Zambonin, *Sens. Actuators B*, 1998, **48**, 363.
11 A. Yassar, J. Roncali and F. Garnier, *J. Electroanal. Chem.*, 1988, **255**, 53.
12 H. Natter and R. Hempelmann, *J. Phys. Chem.*, 1996, **100**, 19525.
13 M. R. Guascito, P. Boffi, C. Malitesta, L. Sabbatini and P. G. Zambonin, *Mater. Chem. Phys.*, 1996, **44**, 17.
14 D. Lu and K. Tanaka, *J. Electrochem. Soc.*, 1996, **143**, 2105.
15 N. Cioffi, C. Di Franco, L. Torsi, L. Sabbatini and P. G. Zambonin, unpublished results.
16 P. E. de Jongh, D. Vanmaekelbergh and J. J. Kelly, *Chem. Commun.*, 1999, 1069.
17 I. Losito and C. G. Zambonin, *J. Electroanal. Chem.*, 1996, **410**, 181.
18 G. Fortier, E. Brassard and D. Belanger, *Biosens. Bioelectron.*, 1990, **5**, 473.
19 N. S. Chang, M. L. Norton and J. L. Anderson, *J. Electrochem. Soc.*, 1991, **138**, 1263.
20 C. Malitesta, I. Losito, L. Sabbatini and P. G. Zambonin, *J. Electron Spectrosc. Relat. Phenom.*, 1995, **76**, 629.
21 C. Malitesta, T. Rotunno, L. Sabbatini and P. G. Zambonin, *J. Chem. Soc., Faraday Trans.*, 1990, **86**, 3607.
22 I. Losito and C. Malitesta, unpublished results.
23 K. L. Tan, B. T. G. Tan, E. T. Kang and K. G. Neoh, *J. Chem. Phys.*, 1991, **94**, 5382.
24 P. Bätz, D. Schmeisser and W. Göpel, *Phys. Rev. B*, 1991, **43**, 9178.
25 A. Milchev, W. S. Kruijt, M. Sluyters-Rehbach and J. Sluyters, *J. Electroanal. Chem.*, 1993, **350**, 89.
26 V. Tsakova and A. Milchev, *J. Electroanal. Chem.*, 1998, **451**, 211.

27 V. Tsakova and D. Borissov, *Electrochem. Commun.*, 2000, **2**, 511.
28 F. Texier, L. Servant, J. L. Bruneel and F. Argoul, *J. Eletroanal. Chem.*, 1998, **446**, 189.
29 R. Kostic, D. Rakovic, S. A. Stepanyan, I. E. Davidova and L. A. Gribov, *J. Chem. Phys.*, 1995, **102**, 3104.
30 J. C. Irwin, J. Charzanowski, T. Wel, D. L. Lookwood and A. World, *Physica C*, 1990, **166**, 456.
31 J. Bukowska and K. Jackowska, *Synth. Met.*, 1990, **35**, 143.
32 C. Di Franco, Graduate thesis, Università degli studi di Bari, Oct. 1999.
33 B. Xu, D. Fichou, G. Horowitz and F. Garnier, *Adv. Mater.*, 1991, **3**, 150.
34 M. Pourbaix, *Atlas of Electrochemical equilibria in aqueous solution*, Pergamon Press, New York, 1966. p. 387.
35 Y. C. Liu and B. J. Hwang, *Thin Solid Films*, 1999, **339**, 233.